Earthquake Geotechnical Engineering for Protection and Development of Environment and Constructions – Silvestri & Moraci (Eds)
© 2019 Associazione Geotecnica Italiana, Rome, Italy, ISBN 978-0-367-14328-2

Lateral and seismic responses of composite caisson-pile foundations

M. Huang & X. Gu
Department of Geotechnical Engineering & Key Laboratory of Geotechnical and Underground Engineering of Ministry of Education, Tongji University, Shanghai, China

W. Tu
School of Civil Engineering and Architecture, East China Jiaotong University, Jiangxi, Nanchang, China

C. Zhang & R. Zhong
Department of Geotechnical Engineering & Key Laboratory of Geotechnical and Underground Engineering of Ministry of Education, Tongji University, Shanghai, China

ABSTRACT: The composite caisson-pile foundation (CCPF) is proposed as the foundation of the highway channel across Qiongzhou Strait in China. A simplified method using a four-spring dynamic Winkler model is developed to evaluate the lateral response of CCPF and the coefficients of the Winkler model are determined based on a modified embedded footing impedance. To analyze the seismic response of the foundation-structure, a simplified model is established, in which the structure is simplified as a lumped mass connected to the foundation with an elastic column. The seismic response of CCPF is analyzed by the proposed simplified method and the results are verified by 3D dynamic finite element simulations. It is found that adding piles under the caisson is an efficient measure to increase the capability of the soil-foundation-structure system subjected to seismic loading. Moreover, dynamic centrifuge tests are also carried out to study the seismic response of CCPF. The test results indicate that for soil with low stiffness adding piles under the caisson can effectively decrease the seismic responses of the foundation and the structure.

1 INTRODUCTION

The composite caisson-pile foundation (CCPF) is proposed as the foundation of the highway channel across Qiongzhou Strait between the mainland and Hainan Island of China in the pre-construction investigation report. The CCPF is a combination of a caisson and grouped piles, as shown in Figure 1. As suggested in the report, the CCPF can be constructed by driving piles from the inside of the caisson after it sinks to the designed depth. It is expected that adding piles beneath the caisson can improve its behavior under lateral and seismic loads.

In the past, caissons are widely used in bridge engineering and offshore engineering (e.g. Jiangyin Yangtze River Highway Bridge in China and San-Francisco-Oakland Bay Bridge in USA), due to their advantages such as the convenience of underwater construction and the good resistance to ship collision. However, compared to the pile group, the embedded depth of the caisson is much shallow, although it is usually categorized as deep foundations. Therefore, attentions should be paid to the performance of caissons under strong lateral or seismic loads, keeping in mind that many structures on caissons suffered serious damages during the Kobe earthquake in 1995 (Gerolymos & Gazetas 2006a). The resistance of the caisson against seismic loads is crucial during the earthquake since the structure inertial may cause large deformation of the foundation. To analyze the dynamic response of a rigid caisson, Gerolymos & Gazetas (2006a) proposed a four-spring Winkler model in which the soil is modeled

with four linear springs associated with dashpot, and a method for determining the spring coefficients based on the impedance of shallow footings was proposed (Gazetas & Tassoulas 1987a, b, Hatzikonstantinou et al. 1989, Fotopoulou et al. 1989, Gazetas 1991). Gerolymos & Gazetas (2006b, c) extended this model for considering the nonlinear behavior of the soil and the interface. In order to achieve reasonable nonlinear hysteric behavior of soil and interface, the beam on a nonlinear Winkler foundation (BNWF) analysis method became the most common approach which extended the linear Winkler model (El Naggar & Novak 1995, El Naggar et al. 2005). In order to back-calculate the Winkler spring coefficients in layered soils, Varun et al. (2009) and Varun (2006) performed numerical simulations using finite element method. Considering the caisson-supported structure, Tsigginos et al. (2008) investigated the seismic response of the foundation-structure system using a dynamic Winkler model for the foundation. Despite insufficient published research on caissons, the abundant references on the shallow embedded foundations can enlighten the study on caissons(Gazetas & Tassoulas 1987a, b, Hatzikonstantinou et al. 1989, Fotopoulou et al. 1989, Gazetas 1991).

Since the CCPF is composed of a caisson and a pile group, its analysis is somewhat complex due to a significant difference between the caisson and the piles. Considering its geometry characteristics, it is reasonable to assume the caisson as a rigid body. However, piles are totally different, owing to not only their slenderness but also the interaction among the individual piles. The dynamic response of pile groups were well studied in the past decades. Simplified methods were developed by Gazetas & Makris (1991), Makris & Gazetas (1992) and Mylonakis & Gazetas (1999) for the axial, lateral, as well as seismic response of pile groups. These simplified methods can be divided into two categories according to the selection of backbone curves: directly use empirical p-y curves (El Naggar & Novak 1996, Allotey & El Naggar 2008) and use the stress-strain curves to derive p-y curves (Heidari et al. 2013, 2014). On the other hand, it must be conducted in the time domain during the nonlinear dynamic response analysis, especially in analyzing the transient dynamic response or seismic response. However, all the analytical procedures of a single pile or pile groups mentioned above were not rigorously developed in the time domain due to frequency-dependence of stiffness and damping parameters. A time domain Winkler model was developed for the axial and flexural response analysis of a single pile subjected to dynamic transient loading by Nogami & Konagai (1986, 1988), and then Konagai & Nogami (1987) extended the approach to obtain a closed form expression of the time domain dynamic soil-pile interaction force for the axial pile groups motion. Nevertheless, the approaches to calculate axial response of pile groups were based on the hypothesis of a polynomial form pile displacement. It may be a crude approximation in terms of the actual deformation.

For seismic problems, to study the foundations solely is not always permissible, because the inertial effect of the superstructures can cause large deformations of the foundation and such interaction should not be ignored. Foundation-superstructure interactions have been widely investigated from experiments to theoretical analyses in the past. Wilson (1998), Boulanger et al. (1999) and Curras et al. (2001) carried out centrifuge tests on seismic responses of pile foundations, in which the superstructures were well designed and considered. The centrifuge tests by Deng et al.(2012) on the seismic response of the bridge also considered the interaction between the soil, foundation and bridge structure. Numerical studies of Wu & Finn (1997), Padrón et al. (2011), Guin & Banerjee (1998) also took the structures into consideration. Stewart et al. (1999a, b) studied the seismic interaction of soil-structure with an analytical method, and the findings were adopted to evaluate the soil-structure interaction of several buildings. In soil-structure interaction, the method of distinguishing kinematic and inertial responses was initially proposed by Kausel et al. (1978), and then followed by many researches such as Mylonakis et al. (1997, 2006) and Tsigginos et al. (2008). A simplified model for the CCPF-structure system in frequency domain was proposed by Zhong & Huang (2013), in which the structure is simplified as a lumped mass and an elastic column connected to the CCPF. With Fast Fourier Transformation (FFT) and inverse Fast Fourier Transformation (iFFT), this simplified model is enabled to solve transient seismic problems.

In this study, the works on the lateral and seismic responses of CCPF as well as CCPF-structure are reviewed. A simplified method with a dynamic Winkler model is introduced first to evaluate the lateral response of CCPF and the coefficients of the four-spring Winkler

model for the caisson are determined. Meanwhile, a simplified model is also established to analyze the seismic response of the foundation-structure, in which the structure is simplified as a lumped mass connected to the foundation with an elastic column. The results are verified by 3D dynamic finite element simulation with domain reduction method. Moreover, dynamic centrifuge tests were also carried out to study the seismic response of CCPF and the effect of piles under the caisson were investigated.

2 LINEAR ANALYSES OF THE LATERAL RESPONSE OF CCPF

A dynamic Winkler model could be established by simplifying the soil resistances using a series of springs (associated with dashpots) for the lateral response of CCPF, as shown in Figure 1(a). The lateral equilibrium equation of the CCPF can be expressed as

$$\mathbf{K_{cp}} \begin{Bmatrix} u_b \\ \theta \end{Bmatrix} = \mathbf{P_b} \tag{1}$$

where u_b and θ are the horizontal displacement and the rotation angle of the base center of the caisson, and $\boldsymbol{P}_\mathbf{b}$ is the load vector given by

$$\mathbf{P_b} = \begin{Bmatrix} Q_0 \\ DQ_0 + M_0 \end{Bmatrix} \tag{2}$$

where D is the length of the caisson part, and Q_0 and M_0 are the dynamic horizontal force and moment applied on the top of the CCPF respectively.

$\mathbf{K_{cp}}$, the impedance matrix of the CCPF with respect to the caisson base center is the combination of the impedance matrices of the caisson and the pile group as

$$\mathbf{K_{cp}} = \mathbf{K_c} + \mathbf{K_p} \tag{3}$$

where $\mathbf{K_p}$ and $\mathbf{K_c}$ are the impedance matrices of the pile group and the caisson respectively.

For the caisson subjected to dynamic lateral force Q_0 and moment M_0, the effect of surrounding soil can be modeled by a four-spring Winkler model proposed by Gerolymos & Gazetas (2006a), as shown in Figure 1(b). Considering the equilibrium with respect to the caisson base center, the response of the caisson can be given by

$$\mathbf{K_c} \begin{Bmatrix} u_b \\ \theta \end{Bmatrix} = \mathbf{P_b} \tag{4}$$

$$\mathbf{K_c} = -\omega^2 \mathbf{M_b} + \mathbf{K_b} \tag{5}$$

where ω is the circular frequency, u_b is the horizontal displacement of the base center, θ is the rotation angle, and $\mathbf{M}_\mathrm{b}$ and $\mathbf{K}_\mathrm{b}$ are the mass matrix and complex stiffness matrix whose details of derivation can be found in Zhong & Huang (2013).

Regarding the piles under the caisson, it is essential to couple the axial vibration into lateral vibration since the piles will deform vertically once the CCPF rotates, as shown in Figure 1(c). In the figure, V^G, H^G and M^G represent the vertical load, horizontal load and moment applied on the pile group, while w^G, u^G and θ^G represent vertical displacement, horizontal displacement and rotation angle of the cap, respectively.

Considering the pile-pile axial interaction and pile-pile lateral interaction, the overall equation for axial-lateral coupled vibration of pile group can be expressed as (Zhong & Huang 2013)

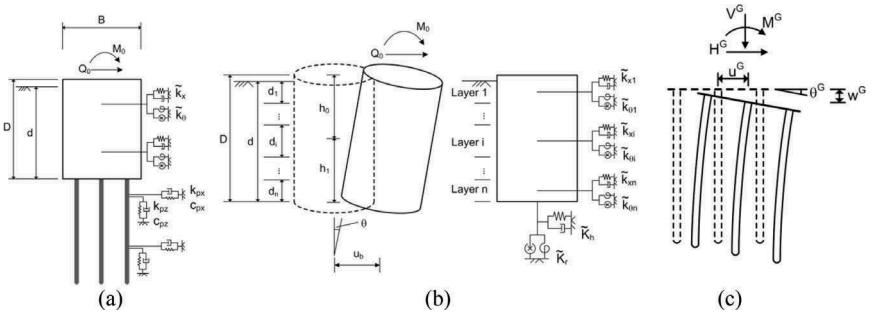

Figure 1. Winkler models for lateral responses of (a) CCPF; (b) caisson; (c) pile groups with rigid cap (from Zhong & Huang 2013).

$$\begin{bmatrix} \mathrm{O} & \mathrm{A}_{12} & \mathrm{A}_{13} & \mathrm{A}_{14} \\ \mathrm{A}_{21} & \mathrm{A}_{22} & \mathrm{A}_{23} & \mathrm{O} \\ \mathrm{A}_{31} & \mathrm{A}_{32} & \mathrm{A}_{33} & \mathrm{O} \\ \mathrm{A}_{41} & \mathrm{O} & \mathrm{O} & \mathrm{A}_{44} \end{bmatrix} \begin{Bmatrix} \mathbf{u^G} \\ \mathrm{H} \\ \mathrm{M} \\ \mathrm{V} \end{Bmatrix} = \begin{Bmatrix} \mathbf{P^G} \\ \mathbf{O} \\ \mathbf{O} \\ \mathbf{O} \end{Bmatrix} \tag{6}$$

where $\boldsymbol{u}^{\mathbf{G}}$ and $\boldsymbol{P}^{\mathbf{G}}$ are the displacement and external force vectors, which are

$$\mathbf{u^G} = \begin{Bmatrix} u^G \\ \theta^G \end{Bmatrix} \tag{7}$$

$$\mathbf{P^G} = \begin{Bmatrix} H^G \\ M^G \end{Bmatrix} \tag{8}$$

H, M, V and A_{12}~A_{44} are vectors of the horizontal force, moment and vertical force applied on the pile and the coefficients of interaction. Details of these can be found in Zhong & Huang (2013).

Finally, the lateral impedance matrix of the pile group can be derived as

$$\begin{aligned} \mathbf{K_p} = &\left(\mathbf{A_{12}} - \mathbf{A_{13}}\mathbf{A_{23}^{-1}}\mathbf{A_{22}}\right)\left(\mathbf{A_{32}} - \mathbf{A_{33}}\mathbf{A_{23}^{-1}}\mathbf{A_{22}}\right)^{-1}\left(\mathbf{A_{33}}\mathbf{A_{23}^{-1}}\mathbf{A_{21}} - \mathbf{A_{31}}\right) \\ &- \mathbf{A_{13}}\mathbf{A_{23}^{-1}}\mathbf{A_{21}} - \mathbf{A_{14}}\mathbf{A_{44}^{-1}}\mathbf{A_{41}} \end{aligned} \tag{9}$$

Figure 2 shows the dynamic lateral response of caisson without or with a 3×3 pile group. To investigate the effect of pile length, the length of the pile varies from 10, 20, 40 to 60m. As

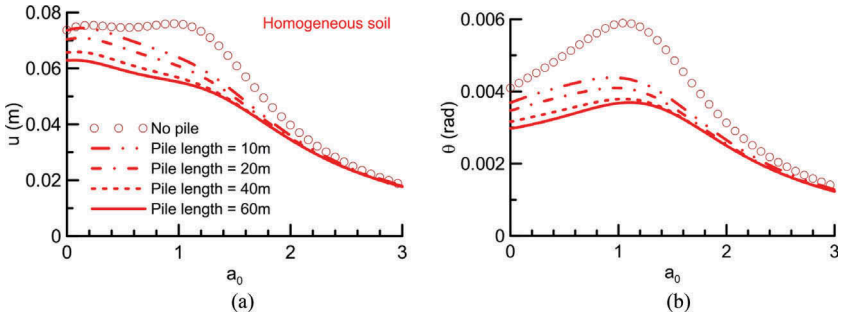

Figure 2. (a) Horizontal displacements and (b) rotation angles of the CCPF in homogeneous soils (from Zhong & Huang 2013).

seen in Figure 2, the presence of piles significantly increases the lateral resistance of the foundation. The lateral displacement and rotation angle of the foundation decreases significantly by the piles beneath the caisson. Meanwhile, the increase of impedance and the decrease of displacement becomes small as the pile length increases. It indicates that the impedance of the foundation cannot be effectively increases with increasing length when the pile length reaches a certain value.

3 LINEAR ANALYSES OF THE SEISMIC RESPONSE OF CCPF - STRUCTURE

Regarding linear elasticity, Kausel et al. (1978) proposed a simplified method for analyzing the seismic response of a soil-foundation-structure system which can be divided into two parts, including kinematic response and inertial response. For a CCPF-structure shown in Figure 3(a), the analysis of kinematic response includes the determination of the displacements and rotation angles of free field (u_{ff}, θ_{ff}) during S-wave propagation, and the determination of kinematic response of the CCPF (u_k, $\dot{k}$) without considering its mass. Meanwhile, the analysis of inertial response includes the calculation of the lateral impedance of the massless CCPF, $\mathbf{R_{HV}}$, and the analysis of the simplified model for the CCPF-column-structure seismic response with u_k and θ_k as excitation, in which the mass of the CCPF is now included.

Figure 3(b) shows the simplified model for foundation-structure interaction, in which the structure is simplified as a lumped mass and an elastic column connected to the foundation, and the foundation is represented by mass matrix with lateral impedance. The lateral impedance matrix of the CCPF, $\mathbf{R_{HV}}$, can be determined with the method proposed in the previous section. Here $\mathbf{R_{HV}}$ has two small differences from $\mathbf{K_{cp}}$. First, it does not contain the mass of the foundation (the mass of the foundation is considered by $\mathbf{m_{bb}}$), and second it is with respect to the caisson top center rather than to the base center like $\mathbf{K_{cp}}$. Therefore, the value of $\mathbf{R_{HV}}$ could be easily obtained using a coordinate transformation based on massless $\mathbf{K_{cp}}$.

Excited by the kinematic displacements u^{KI} and θ^{KI}, the CCPF-structure will have lateral vibrations. If we define u_s and θ_s, u_b and θ_b as the horizontal displacement and rotation angle of the structure and the foundation respectively, the equilibrium condition gives the equation as

$$\begin{Bmatrix} u_s \\ \theta_s \\ u_b \\ \theta_b \end{Bmatrix} = \left(\mathbf{K} - \omega^2 \mathbf{m}\right)^{-1} \begin{Bmatrix} 0 \\ 0 \\ \mathbf{R_{HV}} \begin{Bmatrix} u_k \\ \theta_k \end{Bmatrix} \end{Bmatrix} \tag{10}$$

where $\mathbf{K}$ is the stiffness matrix of the system, which can be expressed as

$$\mathbf{K} = \begin{bmatrix} \mathbf{K_{ss}} & \mathbf{K_{sb}} \\ \mathbf{K_{bs}} & \mathbf{K_{bb}} + \mathbf{R_{HV}} \end{bmatrix} \tag{11}$$

and $\mathbf{m}$ is the mass matrix, which can be expressed as

$$\mathbf{m} = \begin{bmatrix} \mathbf{m_{ss}} & \\ & \mathbf{m_{bb}} \end{bmatrix} \tag{12}$$

In Equation (11), $\mathbf{K_{ss}}$, $\mathbf{K_{sb}}$, $\mathbf{K_{bs}}$ and $\mathbf{K_{bb}}$ are the top-top, bottom-top, top-bottom and bottom-bottom stiffness matrices of the elastic column and can be expressed by

$$\mathbf{K_{ss}} = EI \begin{bmatrix} \frac{12}{h^3} & -\frac{6}{h^2} \\ -\frac{6}{h^2} & \frac{4}{h} \end{bmatrix} \tag{13}$$

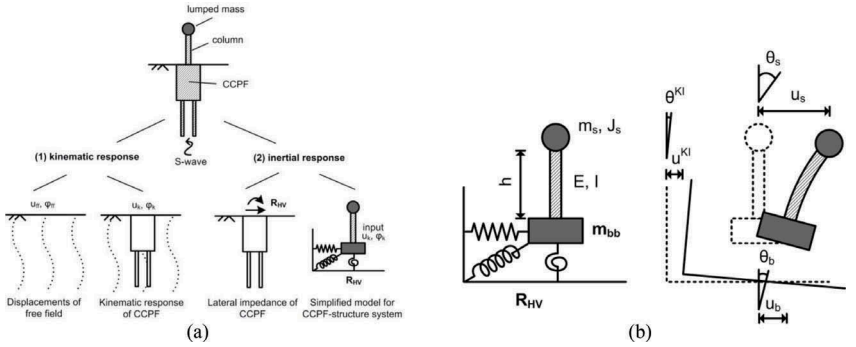

Figure 3. (a) Illustration of the kinematic response and inertial response and (b) a simplified analytical model of a CCPF-structure system(from Zhong & Huang 2014).

$$\mathbf{K_{sb}} = \mathbf{K_{bs}^T} = EI\begin{bmatrix} -\frac{12}{h^3} & -\frac{6}{h^2} \\ \frac{6}{h^2} & \frac{2}{h} \end{bmatrix} \tag{14}$$

$$\mathbf{K_{bb}} = EI\begin{bmatrix} \frac{12}{h^3} & \frac{6}{h^2} \\ \frac{6}{h^2} & \frac{4}{h} \end{bmatrix} \tag{15}$$

In Equation (12), the sub-mass-matrices are

$$\mathbf{m_{ss}} = \begin{bmatrix} m_s & \\ & J_s \end{bmatrix} \tag{16}$$

$$\mathbf{m_{bb}} = \begin{bmatrix} m_c & -h_0 m_c \\ -h_0 m_c & J_c + h_0^2 m_c \end{bmatrix} \tag{17}$$

where E and I are the Young's modulus (complex modulus can be used for considering the structure damping) and moment of inertial of the column cross section, h is the height of column, m_s and J_s are the mass and mass moment of inertial of the superstructure, m_c and J_c are the mass and mass moment of inertial of the foundation, and h_0 is the distance between the center of gravity and the top surface of the foundation.

For a transient seismic problem, the Fourier spectrum, $a_{ff0}(\omega)$-ω relation where $a_{ff0}$is a complex value, can be obtained by FFT analysis of the time history of the input motion. Then the displacement spectrum is calculated by

$$u_{ff0}(\omega) = -\frac{a_{ff0}(\omega)}{\omega^2} \tag{18}$$

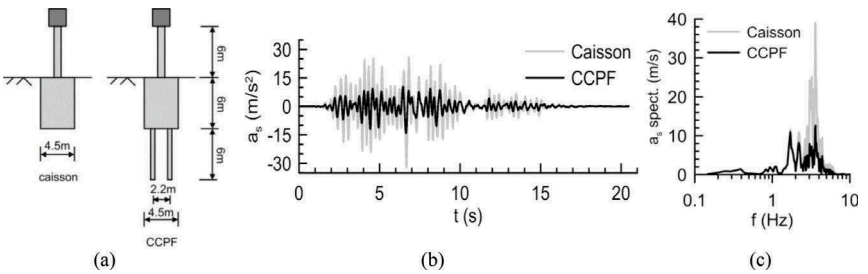

Figure 4. (a) CCPF-structure model; (b) time history of the acceleration of the superstructure; (c) acceleration spectrum of the super structure (from Zhong & Huang 2014).

Thus, one complex value of u_{ff0}can be obtained for each frequency step. After calculations at all frequency steps, the results can be finally transformed into time histories by iFFT.

The seismic response of the CCFP-structure shown in Figure 4(a) is analyzed by the proposed simplified method. The time history of acceleration and the acceleration spectrum of the superstructure with and without piles are shown in Figure 4(b) and Figure 4(c), respectively. The comparison indicated that the acceleration of the superstructure is significantly reduced due to the presence of pile group, especially the components at 3-4 Hz.

4 NONLINEAR ANALYSIS OF THE LATERAL AND SEISMIC RESPONSES OF CCPFIN FREQUENCY DOMAIN

In practical engineering, dynamic response is a typical nonlinear problem due to strain-dependent soil modulus and damping ratio. In general, a reduction factor of soil properties is used in the linear analysis to account for the effect of soil nonlinearity, which is a rough approximation method. Here, the Hardin-Drnevich model (Hardin & Drnevich 1972) is used for the nonlinear analysis as

$$\frac{G}{G_0}=\frac{1}{1+\gamma\gamma_r} \qquad \text{and} \qquad D_s=D_{smax}(1-GG_0) \tag{19}$$

where G is the secant shear modulus of the soil at shear strain γ, γ_γ is the reference shear strain defined as $\gamma_\gamma=\tau_{\max}/G_0$ where $\tau_{\max}$ is the shear strength, G_0 is the initial shear modulus, D_s is the damping ratio at shear strain γ, and D_{smax} is the maximum damping ratio, respectively. For sand, according to the Mohr-Coulomb theory

$$\tau_{\max}=\frac{1}{2}\sigma_v'\left[\tan^2\left(45^\circ+\frac{\varphi'}{2}\right)-1\right]\cos\varphi' \tag{20}$$

where $\varphi'$is the effective angle of internal friction of soil and σ_v' is the vertical effective stress.

The average shear strain in the soil around the pile can be approximated by (Kagawa& Kraft1980)

$$\gamma=\frac{1+\upsilon}{2.5d_0}y \tag{21}$$

where υ is the Poisson's ratio of soil, d_0 is the pile diameter, and y is the pile displacement.

For the dynamic Winkler model, all the stiffness of distributed springs along the caisson and pile shaft are closely related to the soil shear modulus and damping ratio. Therefore, the modified soil parameters can be directly implemented to the dynamic Winkler model to account for the nonlinear soil characteristics, and the response can be solved by iteration.

To illustrate the effect of soil nonlinearity, a CCPF with eight piles is used for analysis. The layouts of CCPF can be seen in Tu et al. (2015). As the dynamic response of foundation is affected by the load magnitude, three different load conditions have been discussed for nonlinear dynamic analysis. Here, soil modulus is recommended to consider the effect of depth or confining pressure (Hardin& Black 1968, Yang & Gu 2013), given by

$$G_0=6908\frac{(2.17-e)^2}{1+e}((1+2K_0)\gamma' h/3)^{0.5} \tag{22}$$

where e, K_0, $\gamma'$and h are the void ratio, coefficient of lateral earth pressure at rest, soil gravity and the embedded depth, respectively.

Figure 5 compares the horizontal dynamic impedance and horizontal displacements of the CCPF when the load magnitude equals 100MN,250MN and 500MN. The results indicate that

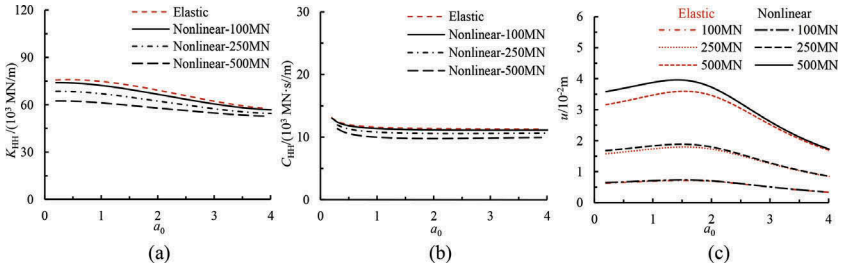

Figure 5. Dynamic responses of CCPF: (a) stiffness; (b) damping; (c) horizontal displacement.

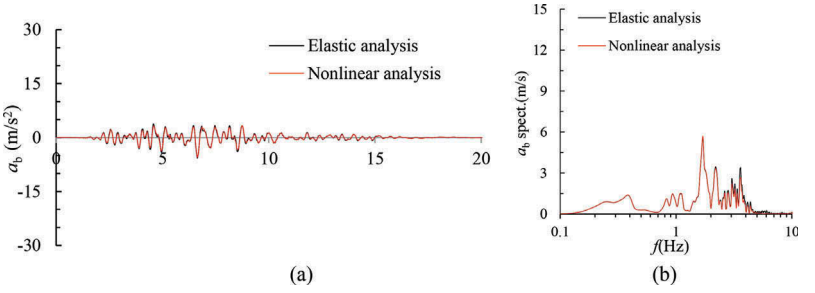

Figure 6. (a) Acceleration time histories and (b) acceleration amplitude spectrum at the superstructure.

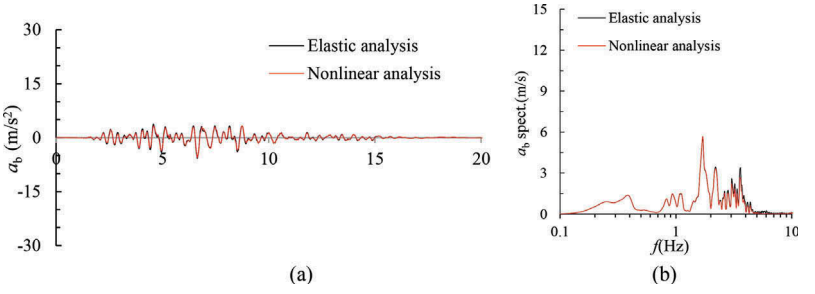

Figure 7. (a) Acceleration time histories and (b) acceleration amplitude spectrum at the foundation.

the reduction in dynamic stiffness is obvious due to the soil nonlinearity when compared to the elastic case. Meanwhile, the stiffness decreases as the applied force increases as expected. As seen in Figure 5(c), the lateral displacement of CCPF increases drastically as load increases. It should be noted that the effect of nonlinearity becomes larger when the applied increases since the strain level increases.

Zhong & Huang (2014) analyzed the seismic response of CCPF with four piles in a relatively soft soil. Details of CCPF structure system and soil properties can be found in the original reference. The acceleration responses without considering and considering soil nonlinearity at the superstructure and foundation are shown in Figures 6 and 7, respectively. As expected, consideration of soil nonlinearity will reduce the acceleration response at the superstructure, and the predominant frequency shifts from high frequency to low frequency. However, the amplitude of reduction is small. Based on the acceleration response of the foundation, the average shear strain of soil around the top of the foundation is calculated to be around 7.3×10^{-4} (Liao& Li 1989). The amplitude of soil nonlinearity is small, which may be the main reason for the small difference between the results of elastic analysis method and nonlinear analysis method.

5 CENTRIFUGE TESTS AND THEORETICAL VERIFICATION

5.1 *Test program and arrangements*

Dynamic centrifuge tests are conducted to investigate the seismic responses of CCPF-structure in sandy silt using the servo-hydraulic shaking table in the geotechnical centrifuge TLJ-150 in Tongji University. All tests were performed at an acceleration of 50g.

The maximum acceleration of the shaking table is 20g, with a maximum time duration of 1s and a frequency range of 20-200 Hz in model scale. The laminar shear box is formed by stacking 22 lightweight aluminum alloy rectangular frames on a base plate and has an internal dimension of 0.5m×0.4 m×0.5m in length, width and height, as shown in Figure 8(a). All frames are separated by ball bearings and the maximum relative horizontal motion between each other is 5mm. The laminar box is used to simulate one-dimensional dynamic site response condition and free boundary conditions, because it eliminate extra shear wave propagation reflected from container walls.

A simulated moderate seismic record often used in Shanghai for the design of critical infrastructure is adopted as the base input motion. The measured prototype acceleration time histories applied to the base is given in Figure 8(b), with a peak acceleration of 0.34g, which was high-pass filtered due to the frequency capacity of shaking table. The record time is 10 seconds longer than the input seismic wave of 20s, for the natural vibration response after earthquake is also of interest in this study. To assess the effect of frequency on the soil-foundation-structure interaction, four main peak frequencies (i.e. 0.391, 1.123, 1.709, 3.613Hz) of input seismic wave are identified as 1 to 4 in the spectral acceleration, as shown in Figure 8(c).

The schematic layouts for the three tests are presented in Figure 9, in which all dimensions are given in prototype scale. It can be seen that a single pile also exists in the tests with a caisson and the composite foundation in order to provide a more convincing reference. Accelerometers are attached at the soil base, soil surface, the foundation surface and the structure. Strain gauges are attached on the beams. Four horizontal displacement sensors are attached to the frames of the container. For simplicity, only the acceleration time history results for the latter two tests are given.

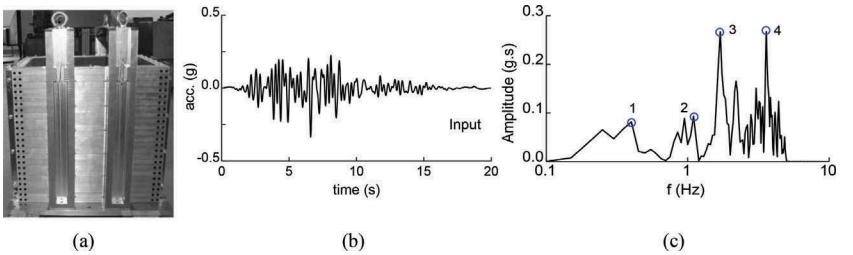

Figure 8. (a) Laminar box; (b) the input acceleration time history; (c) the acceleration response spectra.

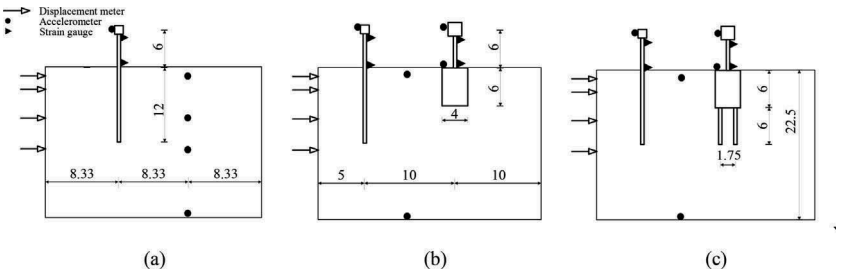

Figure 9. Schematic of test layouts (a) test 1; (b) test 2 - caisson; (c) test 3 - CCPF.

All model piles, caisson and upper structure are fabricated using aluminum alloy. The dimensions of prototype concrete pile are 0.5 m in diameter, 12 m in length and 0.02 m in thickness, resulting in a bending stiffness of $EI = 1.87\times10^8$ Nm^2. The prototype concrete hollow cylindrical caisson is 4m in diameter, 6m in height and 0.3m in thickness, with a lateral moment of inertia of5.207×10^5kgm^2.The 2×2 pile group for the composite foundation has a length of 6mand pile space of 1.75m. The upper structure is modeled as a 1-degree-of-freedom (DOF) system consisting of a beam and a concentrated mass. The connecting beam has the same section as single pile. The cubic mass is acting at a height of 6m above the ground surface. The cube founded on the single pile is 4882.8kg in mass, 1.25m in length, 1271.6 kgm^2 in lateral moment of inertia, and that founded on the caisson and composite foundation is 20000 kg in mass, 2m in length, 133333kgm^2 in lateral moment of inertia.

The model soil is sandy silt in Shanghai, with a coefficient of uniformity (C_u) of 4.5 and median diameter (d_{50}) of 0.065 mm. The tested soil has a water content of 7% and has a density of 1.467g/cm^3. The shear wave velocity V_s of the soil is 66.7m/s considering the stress level in the tests.

5.2 *Test results and comparison with calculations*

Figures 10 and 11 show the acceleration-time histories of soil profiles at the ground base and surface for the two tests using caisson and caisson-piles foundation, respectively. The acceleration-time histories recorded on the upper structure build on reference pile are displayed in Figure 12. Agreements of measured responses of site motion and the upper structure here approved the repeatability and consistency in the centrifuge tests, and no additional motions has been triggered. According to Figures 10 and 11, acceleration is diminished as the waves

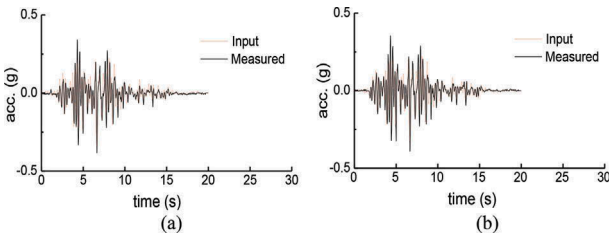

Figure 10. Acceleration time histories of free field soil at ground base: (a) test 2; (b) test 3.

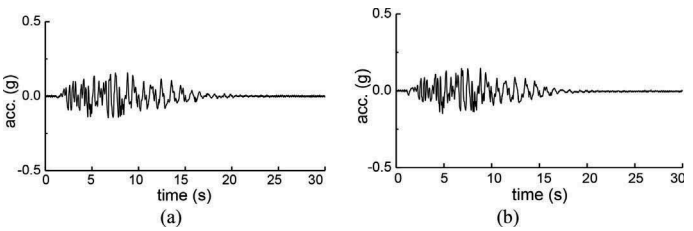

Figure 11. Acceleration time histories of free field at soil surface: (a) test 2; (b) test 3.

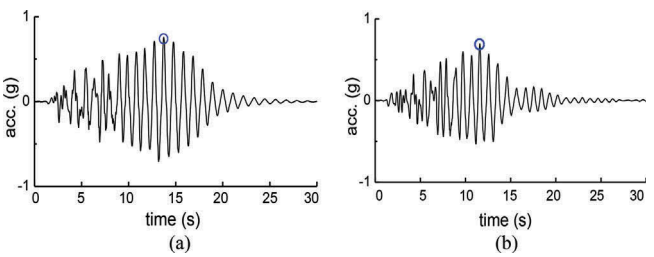

Figure 12. Acceleration time histories of upper structure on single pile: (a) test 2; (b) test 3.

pass through the soil layer, the maximum peak of which were 0.38g at ground base and decreased to 0.16g and 0.15g at soil surface, attributing to the limited natural frequency of soft soil for the tests. In Figure 6, the acceleration of upper-structure was augmented compared to the input base motion in Figure 10. Based on the time history in Figure 10, the main input excitation occurs in the first 10s, resulting in a forced vibration of the pile-soil-upper structure system in this stage. Then the system responded in a free vibration, behaving as a smooth shape of the time history in Figure 12. It should be noted that the maximum peak acceleration of upper structure exists at 14s and 13 s respectively in free vibration, out of phase with the excitation-time history. This is because the structure absorbed energy during the first 10s seismic excitation. Hence, between 10s and 13s (or 14s), in spite of limited excitation according to acceleration-time history at base, the energy supply in the system continues and the rate of supply is larger than that of dissipation. Therefore, the vibration was enhanced, resulting in a maximum acceleration at 14s and 13s respectively. The time history in Figure 12 presents a damped free vibration of upper structure.

Figures 13 and 14 illustrate the time-histories of upper structure and foundation supported by caisson and caisson-piles. By comparing with the time histories of upper structure build on reference pile in Figure 12, it can be seen that the responses of upper structure build on single pile are obviously different from that build on caisson in Figure 13(a) and on caisson-piles in Figure 13(b). The maximum acceleration of upper structure occurs at 7s in the stage of forced excitation and the following free vibration begins at 17s. It can be explained that the rigidity of caisson and caisson-piles are much larger than that of single pile, which limited the free vibration of soil foundation and upper structure system.

Figure 15 presents the amplifications of acceleration in the soil layer, foundation and upper structure subjected to seismic excitation. Amplifications were obtained by normalizing maximum acceleration at different elevations based on the maximum base acceleration in Figure 15(a) and based on the maximum ground surface acceleration in Figure 15(b). Evidently, accelerations diminished from the base to the soil surface and then augmented from the soil surface to the upper structure. Small discrepancies exists for the amplification across the soil layer for the two tests in Figure 15(a). Considering the perfect repeatability of soil layer in test soil preparation is impossible, the small error is acceptable. The normalization in Figure 15(b), excluding the error in soil preparation, shows that the acceleration amplification of upper structure founded on caisson-piles foundation is obviously lower than that on caisson

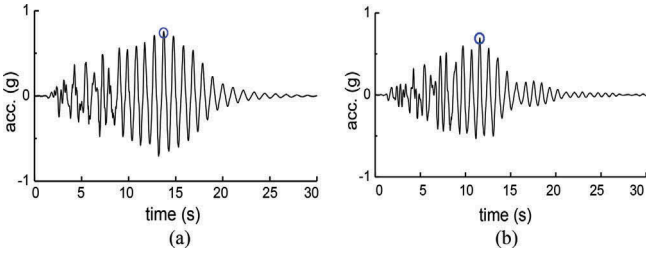

Figure 13. Acceleration time histories of the upper structure: (a) caisson (test 2); (b) CCPF (test 3).

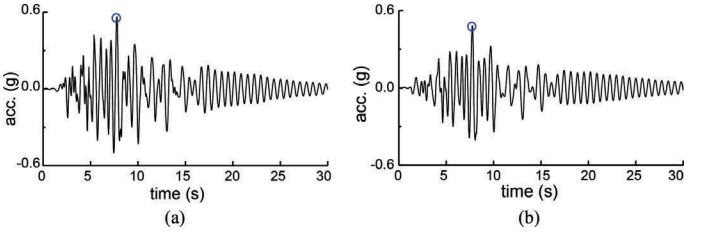

Figure 14. Acceleration time histories of the foundation: (a) caisson (test 2); (b) CCPF (test 3).

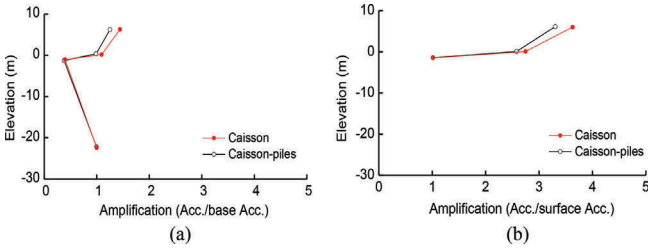

Figure 15. Amplifying of acceleration in soil layer, foundation and upper structure: based on (a) base acceleration and (b) surface acceleration.

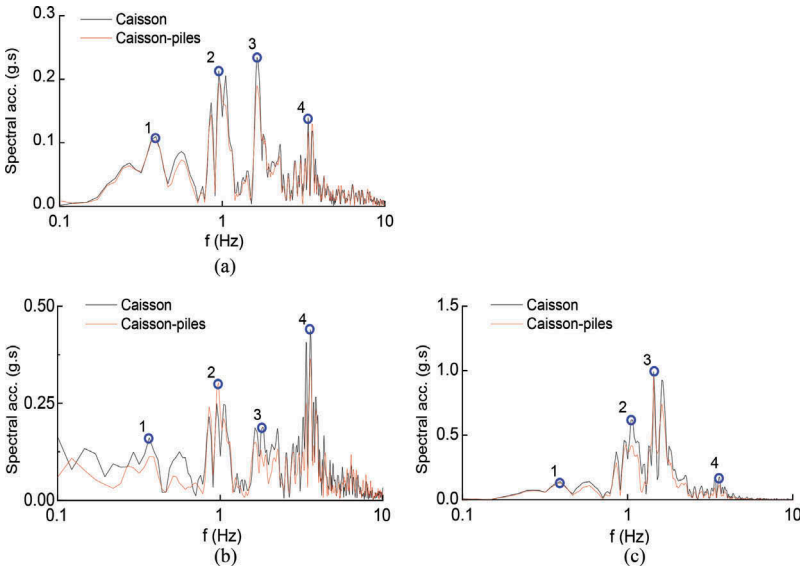

Figure 16. Fourier amplitude spectra of acceleration-time histories: (a) soil surface; (b) foundation; (c) upper structure.

foundation, which proved the effectiveness of caisson-piles foundation in supporting upper structure in seismically active regions.

Figure 16 shows the Fourier amplitude spectra of surface soil, foundation and upper structure in the two tests, in which the four main peak frequencies of input seismic wave are labeled. Obviously, the maximum of the Fourier amplitude can correspond to the fundamental frequency of related items. According to Figure 16(c), the first and second maximum Fourier amplitudes of input seismic wave are at frequencies 3 and 4, while Figure 16(a) shows that the first and second amplitude of surface soil are at frequencies 2 and 3. This means the fundamental frequency of soil is approximate to the frequency 2. In Figure 16(b), the maximum Fourier amplitude of foundation is observed at frequency 4, and that of upper structure is observed at frequency 3 in Figure 16(c), which demonstrates that the fundamental frequency of upper structure and foundation are close to frequency 4 and 3 respectively. Furthermore, as can be seen in Figure 16(b), frequencies 2 and 4 correspond to the first and second maximum Fourier amplitude for caisson and caisson-piles foundation. The comparisons of them reveal that the amount of maximum amplitude for caisson at frequency 4 is higher than the value at frequency 2. However, they are approximately the same value for caisson-piles foundation. The natural frequency of the foundation is sensitive to additional pile groups at caisson bottom, which attributes to the elimination of possible resonance effect at frequency 4.

Table 1. Comparisons of peak accelerations between tests and calculation.

	Structure accelerations (m/s^2)			Foundation accelerations (m/s^2)		
	Tests	Linear	Nonlinear	Tests	Linear	Nonlinear
Caisson	0.565	0.815	0.766	0.428	0.159	0.496
Caisson-piles	0.484	0.599	0.544	0.381	0.141	0.461

To validate the numerical methods introduced above in analyzing the seismic response of the soil-foundation- upper structure system, the centrifuge tests for caisson and caisson-piles are calculated considering linear and nonlinear soil response. Comparisons of maximum acceleration of upper structure and foundations (caisson and caisson-piles) are made between the test results and calculated results. As shown in Table 1, compared to linear calculation, the nonlinear analysis always gives better estimations of peak upper structure acceleration and peak foundation acceleration, no matter the upper structure is built on caisson or on caisson-piles, which reveals that the ground motion amplitudes in the tests result in considerable soil nonlinear response, and the nonlinear numerical simulation is acceptable in calculating this problem. Since the formation of a gap is observed between foundation and surrounding soil in centrifuge tests, which is not accounted for in numerical simulation, the peak accelerations were slightly overestimated in all cases for nonlinear analysis.

6 NONLINEAR ANALYSIS IN TIME DOMAIN FOR LATERAL RESPONSE OF CCPF

The actual interactions between CCPF and soil involve complicated material and geometric nonlinearity such as soil plasticity, separation, slippage and strong interface nonlinearity while foundations under moderate and strong seismic loading or other excitation. To obtain such nonlinear response, several parameters have been modified as follows

Extended Masing's rules are used in modeling oval-shaped hysteresis loops (Pyke 1979)

$$\kappa = 1 \pm \frac{p_{ur}}{\delta_q p_f} \tag{23}$$

where κ is the Pyke's scaling parameter, the plus and minus signs denote unloading and reloading, respectively, p_{ur} is the current soil reaction at the onset of unloading or reloading, $p_f$is the ultimate lateral soil reaction, and δ_q is a strength degradation factor.

Cyclic degradation or hardening mechanisms given by (Huang & Liu 2015)

$$\delta_\varsigma = \delta_{\varsigma res} + (1 - \delta_{\varsigma res}) e^{-b\varepsilon^p} \tag{24}$$

where b is a material parameter, reflecting the rate of degradation with accumulative strain. δ_ζ stands for the degraded strength factor or δ_q or stiffness degradation factor δ_E, respectively. $\delta_{\zeta res}$ are defined as the residual strength ratio δ_{qres} or residual stiffness ratio δ_{Eres}.

The accumulative equivalent plastic strain ε^p can be replaced by the accumulative equivalent plastic displacement. The accumulative equivalent plastic displacement at Mth cycle can be expressed as

$$\mathrm{y}_p = \sum \Delta \mathrm{y}_{\mathrm{pi}} \ (i = 1,\ 2, 3, \cdots 2M - 1, 2M) \tag{25}$$

where Δy_{pi} is the equivalent plastic displacement at the ith cycle, and theΔy_{p1} andΔy_{p2} are shown in Figure 17.

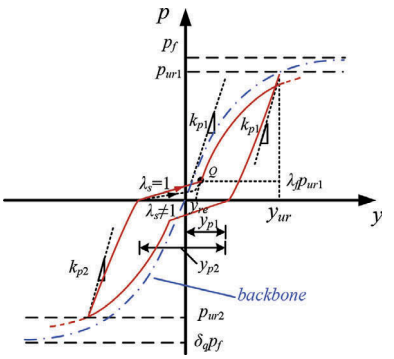

Figure 17. Schematic of unloading and reloading curves (from Huang et al. 2018).

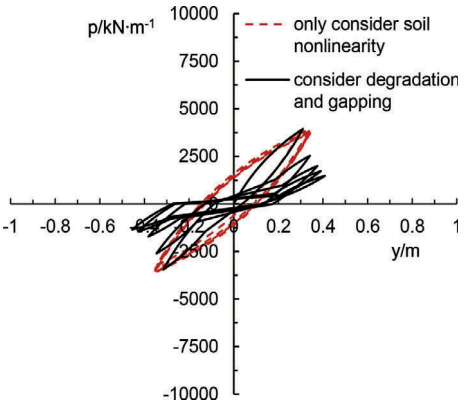

Figure 18. Comparison of the horizontal soil reaction-displacement loops at the selected depth z=10m (from Huang et al. 2018).

Radiation damping of soil is always frequency-dependent which cannot be applied in the time domain directly. However, Berger et al. (1977) recommended the following approximate equation for the radiation damping, thanks to its simplicity and frequency-independent

$$c_{\mathrm{h}} = 4d_0\rho V_s \tag{26}$$

where ρ is the density of soil,d_0 is the pile diameter, and V_s is the shear wave velocity of soil.

Then, combined with the dynamic equilibrium equations of pile groups and caisson foundation, the dynamic response of CCPF with respect to the base center of the caisson part can be solved by the Newmark-β method with linear acceleration assumption.

Huang et al. (2018) analyzed the lateral response of CCPF with 9 piles. Details of CCPF and soil properties can be found in the original reference. Take the dynamic response of CCPF at f=0.1Hz as an example, soil gaping and degradation show a significant effect on the displacement of foundation in the subsequent cycles as shown in Figure 18. Inspecting the results, the hysteresis loops of soil reaction begin to change shapes from a slightly oval-shaped to s-shaped, especially around the upper part of the caisson body.

7 CONCLUSIONS

In this study, the linear and nonlinear lateral response of CCPF were analyzed using a dynamic Winkler model. Meanwhile, the linear and nonlinear seismic response of CCPF-structure in

frequency domain were also investigated. The results of the numerical analyses were compared with those in centrifuge tests. Finally, the nonlinear analysis of the CCPF subjected to cyclic loading in time domain was carried out. The main conclusions can be summarized as follows:

1. A simplified four-spring Winkler model for the caisson was proposed and their coefficients were determined. It shows that it is very important to account for the difference of rotational embedded impedance between the footing and the caisson. The results also showed that adding piles under the caisson is an efficient measure to increase the lateral capability of the CCPF.
2. The lateral response of the CCPF indicated that it is important to account for the nonlinear interaction between soil-structure. The effect of soil nonlinear behavior becomes more significant as the external load increases.
3. A simplified model is established, in which the structure is simplified as a lumped mass connected to the foundation with an elastic column and the transient seismic foundation-structure interaction was solved by Fast Fourier Transformation. It was of found that soil nonlinearity will result in a reduction in the acceleration response at the superstructure, and the predominant frequency is shifted from high frequency to low frequency. However, the amplitude of reduction is small in the analyzed case which is probably resulted from the small average shear strain.
4. The centrifuge test results indicated that it is essential to account the nonlinear behavior in numerical analyses. Compared to nonlinear calculation, the linear analysis always gives larger peak acceleration of upper structure and smaller peak acceleration of foundation. Since the formation of a gap is observed between foundation and surrounding soil in centrifuge tests, which is not accounted for in numerical simulation, the peak accelerations were slightly overestimated in all cases for nonlinear analysis.
5. A method was proposed to investigate the nonlinear lateral response of CCPF in time domain. It was found that soil gaping and degradation show a significant effect on the displacement of foundation subjected to cyclic loads.

ACKNOWLEDGEMENTS

The authors wish to acknowledge the support provided by the National Natural Science Foundation of China (Grant Nos. 51822809 and 51579177), the National Basic Research Program of China (973 Program) (Grant No. 2013CB036304) and Fundamental Research Funds for the Central Universities. These supports are gratefully acknowledged.

REFERENCES

Allotey, N. & El Naggar, M.H. 2008. Generalized dynamic Winkler model for nonlinear soil-structure interaction analysis. *Canadian Geotechnical Journal* 45(4): 560–573.

Berger, E., Mahi, S.A. & Pyke, R. 1977. Simplified method for evaluating soil-pile-structure interaction effects, *Proc. of the 9th offshore Technology Conference, January 1977*. Texas: Houston.

Boulanger, R.W., Curras, C.J., Kutter, B.L., Wilson D.W. & Abghari, A. 1999. Seismic soil-pile-structure interaction experiments and analyses. *Journal of Geotechnical and Geoenvironmental Engineering* 125(9):750–759.

Curras, C.J., Boulanger, R.W., Kutter, B.L., Wilson D.W. 2001. Dynamic experiments and analyses of a pile-group-supported structure. *Journal of Geotechnical and Geoenvironmental Engineering* 127(7):585–596.

Deng, L., Kutter, B. & Kunnath, S. 2012. Centrifuge modeling of bridge systems designed for rocking foundations. *Journal of Geotechnical and Geoenvironmental Engineering* 138(3):335–344.

El Naggar, M.H. & Novak, M. 1996. Nonlinear analysis for dynamic lateral pile response. *Soil Dynamics and Earthquake Engineering* 15(4): 233–244.

El Naggar, M.H. & Novak, M. 1995. Nonlinear lateral interaction in pile dynamics. *Soil Dynamics and Earthquake Engineering* 14(2): 141–157.

El Naggar, M.H., Shayanfar, M.A., Kimiaei, M. & Aghakouchak, A.A. 2005. Simplified BNWF model for nonlinear seismic response analysis of offshore piles with nonlinear input ground motion analysis. *Canadian Geotechnical Journal* 42(2): 365–380.
Fotopoulou, M., Kotsanopoulos, P., Gazetas, G. & Tassoulas, JL. 1989. Rocking damping of arbitrarily-shaped embedded foundations. *Journal of Geotechnical Engineering, ASCE* 115(4): 473–489.
Gazetas, G. & Makris, N. 1991. Dynamic pile-soil-pile interaction. Part I: Analysis of axial vibration. Earthquake Engineering & Structural Dynamics 20: 115–132.
Gazetas,G. & Tassoulas, J.L. 1987a. Horizontal stiffness of arbitrarily shaped embedded foundations. *Journal of Geotechnical Engineering, ASCE* 113(5): 440–457.
Gazetas,G. & Tassoulas, J.L. 1987b. Horizontal damping of arbitrarily shaped embedded foundations. *Journal of Geotechnical Engineering, ASCE* 113(5): 458–475.
Gazetas, G. 1991. Formulas and charts for impedances of surface and embedded foundations. *Journal of Geotechnical Engineering, ASCE* 117(9): 1363–1381.
Gerolymos, N. & Gazetas, G. 2006a. Winkler model for lateral response of rigid caisson foundations in linear soil. *Soil Dynamics and Earthquake Engineering* 26(5): 347–361.
Gerolymos, N. & Gazetas, G. 2006b. Development of Winkler model for static and dynamic response of caisson foundations with soil and interface nonlinearities. *Soil Dynamics and Earthquake Engineering* 26(5): 363–376.
Gerolymos, N. & Gazetas, G. 2006c. Static and dynamic response of massive caisson foundations with soil and interface nonlinearities-validation and results. *Soil Dynamics and Earthquake Engineering* 26 (5): 377–394.
Guin, J. & Banerjee, P. 1998. Coupled soil-pile-structure interaction analysis under seismic excitation. *Journal of Structural Engineering* 124(4):434–444.
Hardin, B.O. & Black, W.L.. 1968. Vibration modulus of normally consolidated clay. *Journal of the Soil mechanics and Foundations Division* 94(2): 353–370.
Hardin, B.O. & Drnevich, V.P. 1972. Shear modulus and damping in soils: design equation sand curves. *Journal of the Soil mechanics and Foundations Division* 98(7): 667–692.
Hatzikonstantinou, E., Tassoulas, J.L., Gazetas, G., Kotsanopoulos, P. & Fotopoulou, M. 1989. Rocking stiffness of arbitrarily shaped embedded foundations. *Journal of Geotechnical Engineering, ASCE* 115(4): 457–472.
Heidari, M., El Naggar, M.H., Jahanandish, M. & Ghahramani, A. 2014. Generalized cyclic p–y curve modeling for analysis of laterally loaded piles. *Soil Dynamics and Earthquake Engineering*63:138–149.
Heidari, M., Jahanandish, M., El Naggar, M.H. & Ghahramani, A. 2013. Nonlinear cyclic behavior of laterally loaded pile in cohesive soil. *Canadian Geotechnical Journal* 51(2): 129–143.
Huang, M.S. & Liu, Y. 2015. Axial capacity degradation of single piles in soft clay under cyclic loading. *Soils and Foundations* 55(2): 315–328.
Huang, M.S., Tu, W.B. & Gu, X.Q. 2018. Time domain nonlinear lateral response of dynamically loaded composite caisson-piles foundations in layered cohesive soils. *Soil Dynamics and Earthquake Engineering* 106:113–130.
Kagawa, T.& Kraft, L.M. 1980. Lateral load-deflection relationships of piles subjected to dynamic loadings. *Soils and Foundations* 20(4): 19–36.
Kausel, E., Whitman, R.V., Morray, JP.& Elsabee, F. 1978. The spring method for embedded foundations. *Nuclear Engineering and Design* 48: 377–392.
Konagai, K. & Nogami, T. 1987. Time-domain axial response of dynamically loaded pile groups. *Journal of Engineering Mechanics* 113(3): 417–430.
Liao, Z.P. & Li, X.J. 1989. *Seismic Microzonation-Theory and Practice*. Beijing: China Earthquake Press. (in Chinese)
Makris, N. & Gazetas, G.1992. Dynamic pile-soil-pile interaction. Part II: Lateral and seismic response. *Earthquake Engineering &Structural Dynamics* 21: 145–162.
Mylonakis, G. & Gazetas, G. 1999. Lateral vibration and internal forces of grouped piles in layered soil. *Journal of Geotechnical Engineering, ASCE* 125(1): 16–25.
Mylonakis, G., Nikolaou, A. & Gazetas, G.1997. Soil-pile-bridge seismic interaction: Kinematic and inertial effects. Part 1: Soft soil. *Earthquake Engineering &Structural Dynamics* 26(3): 337–359.
Mylonakis, G., Nikolaou, S. & Gazetas, G. 2006. Footings under seismic loading: Analysis and design issues with emphasis on bridge foundations. *Soil Dynamics and Earthquake Engineering* 26(9): 824–853.
Nogami, T. & Konagai, K. 1986. Time domain axial response of dynamically loaded single piles. *Journal of Engineering Mechanics* 112(11): 1241–1252.
Nogami, T. & Konagai, K. 1988. Time domain flexural response of dynamically loaded single piles. *Journal of Engineering Mechanics* 114(9): 1512–1525.

Padrón, L.A., Aznarez, J.J. & Maeso, O. 2011. 3-D boundary element-finite element method for the dynamic analysis of piled buildings. *Engineering Analysis with Boundary Elements* 35(3):465–477.
Pyke, R.M. 1979. Nonlinear soil models for irregular cyclic loadings. *Journal of Geotechnical and Geoenvironmental Engineering*, 715–725.
Stewart, J.P., Fenves, G.L. &Seed R.B.1999. Seismic soil-structure interaction in buildings. I: Analytical methods. *Journal of Geotechnical and Geoenvironmental Engineering* 125(1):26–37.
Stewart, J.P., Seed R.B.& Fenves, G.L.1999. Seismic soil-structure interaction in buildings. II: Empirical findings. *Journal of Geotechnical and Geoenvironmental Engineering* 125(1):38–48.
Tsigginos, C., Gerolymos, N., Assimaki, D. & Gazetas, G. 2008. Seismic response of bridge pier on rigid caisson foundation in soil stratum. *Earthquake Engineering and Engineering Vibration* 7(1): 33–44.
Tu, W.B., Huang, M.S. & Zhong, R. 2015. Scour effects on the dynamic lateral response of composite caisson-piles foundations considering stress history of sand. *Japanese Geotechnical Society Special Publication* 1(6): 23–28.
Varun Assimaki, D. & Gazetas, G. 2009. A simplified model for lateral response of large diameter caisson foundations - Linear elastic formulation. *Soil Dynamics and Earthquake Engineering* 29(2): 268–291.
Varun. 2006. A simplified model for lateral response of caisson foundations. Athens, Greece: Georgia Institute of Technology.
Wilson, D.W. 1998. Soil-pile-superstructure interaction in liquefying sand and soft clay. PhD Thesis, University of California, Davis.
Wu, G. &Finn, W. 1997. Dynamic nonlinear analysis of pile foundations using finite element method in the time domain. *Canadian Geotechnical Journal* 34(1):44–52.
Yang, J. & Gu, X.Q. 2013. Shear stiffness of granular material at small strain: does it depend on grain size? *Geotechnique*63(2), 165–179.
Zhong, R. & Huang, M.S. 2013. Winkler model for dynamic response of composite caisson-piles foundations: Lateral response. *Soil Dynamics and Earthquake Engineering*55:182–194.
Zhong, R. & Huang, M.S. 2014. Winkler model for dynamic response of composite caisson-piles foundations: Seismic response. *Soil Dynamics and Earthquake Engineering*66: 241–251.